Supporting Information to

Chlorine Monoxide (Cl_2O) and Molecular Chlorine (Cl_2) as Active Chlorinating Agents in Reaction of Dimethenamid with Aqueous Free Chlorine

A research article submitted to *Environmental Science and Technology*

*John D. Sivey, Corey E. McCullough and A. Lynn Roberts**
Department of Geography and Environmental Engineering
Johns Hopkins University
313 Ames Hall
3400 North Charles Street
Baltimore, MD 21218

*Corresponding author contact information:

Phone: 410-516-4387; Fax: 410-516-8996; E-mail: lroberts@jhu.edu

Contains 26 pages, including three tables and eight figures.

1. Chemical reagents and suppliers

Unless otherwise specified, all chemicals were of reagent grade purity or greater and were used as received. Sodium nitrate and chloroform-*d* with TMS (1%, v/v) stabilized with silver foil were purchased from Acros; sodium thiosulfate from Alfa Aesar; DPD chlorine indicator solution from Aqua Solutions; dimethenamid (DM) and propachlor from Chem Service; concentrated nitric acid from EMD; sodium hypochlorite (*ca*. 6% w/w), toluene, sodium chloride and methanol from Fisher Scientific; and potassium phosphate (monobasic), sodium acetate (anhydrous), sodium borate decahydrate and sodium hydroxide (2.00 N) from JT Baker.

2. Ion chromatography

Ion chromatographic analyses were performed with a Dionex DX-120 ion chromatograph equipped with a Dionex IonPack® AS14 column (4 x 250 mm). The eluent composition was 3.5 mM Na_2CO_3 and 1 mM $NaHCO_3$.

3. Effects of ionic strength on DM reactions with FAC

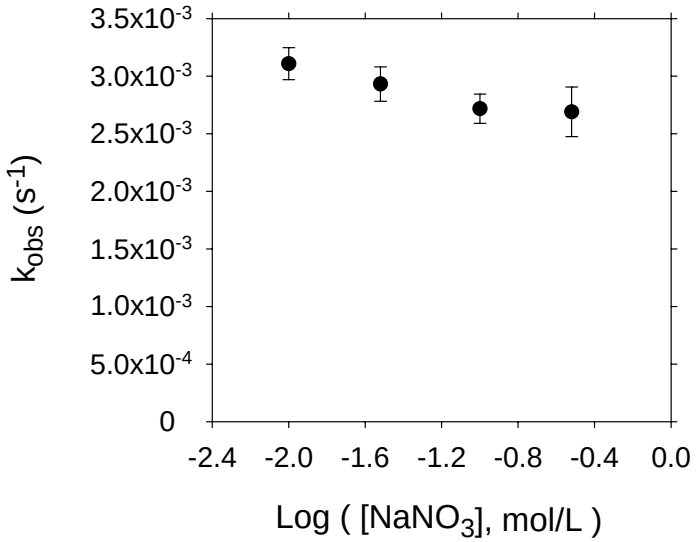

Figure S1. Rate constants for reactions of DM with FAC as a function of $[NaNO_3]$ (note log scale on horizontal axis only). Other conditions: $[FAC]_o = 5 \times 10^{-4}$ M; $[DM]_o = 1.5 \times 10^{-5}$ M; pH = 6.0; [phosphate buffer] = 0.010 M, T = 25.0 ± 0.1°C.

4. GC analytical details

Qualitative analysis via gas chromatography/mass spectrometry (GC/MS) was performed on a Thermo Finnigan Trace GC (2000 Series) interfaced with a quadrupole mass-selective detector (Fisons MD 800). Injection of 2 μL of toluene extract into a programmable temperature vaporizing inlet operated at 240^{o}C in splitless mode preceded analyte separations on an Agilent DB5-MS column (30 m, 0.25 mm i.d., 0.25 μm film thickness) under constant helium flow (1.5 mL/min). An initial oven temperature of 110^{o}C was held for 1 min, followed by a temperature ramp of 10^{o}C/min to 280^{o}C; total run time was 18 min. Following an initial solvent delay of 4.5 min, mass spectra were obtained using electron ionization (70 eV) in full scan mode covering the ion range $11 \leq m/z \leq 399$.

Quantitative analysis via GC interfaced with a micro-electron capture detector (μECD) was performed on an Agilent 7895 GC system. Injection of 2 μL of toluene extract into a split/splitless injector at 250^{o}C preceded analyte separations on an Agilent HP-1 column (30 m, 0.32 mm i.d., 3 μm film thickness) under constant helium flow (1.5 mL/min). The inlet flow was operated in splitless mode for 1 min, followed by a 13:1 split flow for 1 min and a 10:1 split flow thereafter. An initial oven temperature of 200^{o}C was employed, with an immediate ramp of 15^{o}C/min to 260^{o}C, followed by a 9 min hold; total run time was 14 min. The micro-electron capture detector was set to 250^{o}C with 10 mL/min of make-up gas flow (5% methane / 95% argon).

Retention times of each analyte for both the GC/MS and GC/μECD methods are listed in **Table S1**.

Table S1. Retention times of analytes for the GC/MS and GC/μECD analytical methods.

	Retention Time (min)	
Analyte	*GC/MS*	*GC/μECD*
Propachlor (internal standard)	9.4	5.2
DM	11.4	8.1
CDM	14.2	10.0
BDM	16.8	11.9

5. Synthesis and characterization of chlorodimethenamid and bromodimethenamid

Chlorodimethenamid. To a 125-mL Erlenmeyer flask was placed DM (95 μmol) and methanol (30 mL). To this solution was added NaOCl (17 mmol) dropwise with stirring at room temperature. The combined solution was allowed to stir in the dark for 30 min. The solution was transferred to a 125-mL separatory funnel containing 20 mL of toluene and 40 mL of NaCl solution (5% w/v). Following liquid:liquid extraction, the toluene phase was isolated and washed with an additional 40 mL of NaCl solution (5% w/v). The toluene phase was placed in an Erlenmeyer flask, and the solvent was evaporated with forced air at room temperature to yield chlorodimethenamid (CDM, 41 μmol; 43% yield), a clear, colorless liquid.

Bromodimethenamid. To a 125-mL Erlenmeyer flask was placed DM (128 μmol) and methanol (30 mL). To this solution was added dropwise a solution of NaOCl (0.5 mmol), NaBr (0.5 mmol) and HNO_3 (to pH 5.4) with stirring at room temperature. The combined solution was allowed to stir in the dark for 10 min. The solution was transferred to a 125-mL separatory funnel containing 20 mL of NaCl solution (5% w/v). The solution was extracted with toluene (20 mL x 2). The toluene extracts were combined and washed with 25 mL of $NaHCO_3$ solution (5% w/v). The toluene phase was placed in an Erlenmeyer flask, and the solvent was evaporated

with forced air at room temperature to yield bromodimethenamid (BDM, 92 μmol; 72% yield), a clear, colorless liquid.

Characterization of synthesis products. The identity of the products was determined by GC/MS and proton nuclear magnetic resonance spectroscopy (^{1}H NMR), performed in $CDCl_3$ on a Bruker Avance 300 MHz FT-NMR spectrometer. The mass spectrum of CDM was consistent with that reported by Hladik *et al*. (*S1*). The mass spectrum of BDM is shown in **Figure S2**. Fragmentation and isotope patterns are consistent with replacement of H on the thiophene ring of DM with Br. Formation of a brominated product is consistent with the greater retention time observed for this product than for CDM (**Table S1**).

The ^{1}H NMR results for the starting material (DM) and the products (CDM and BDM) are summarized in **Table S2**, with corresponding atom assignments shown in **Figure S3**. Of note is the absence of an aromatic proton signal in the spectra for CDM and BDM, which is present as assignment **h** in the starting material. This finding is consistent with the replacement of the aromatic proton of DM with chlorine or bromine for CDM and BDM, respectively. The purity of both CDM and BDM as determined by GC/MS and ^{1}H NMR exceeded 99%.

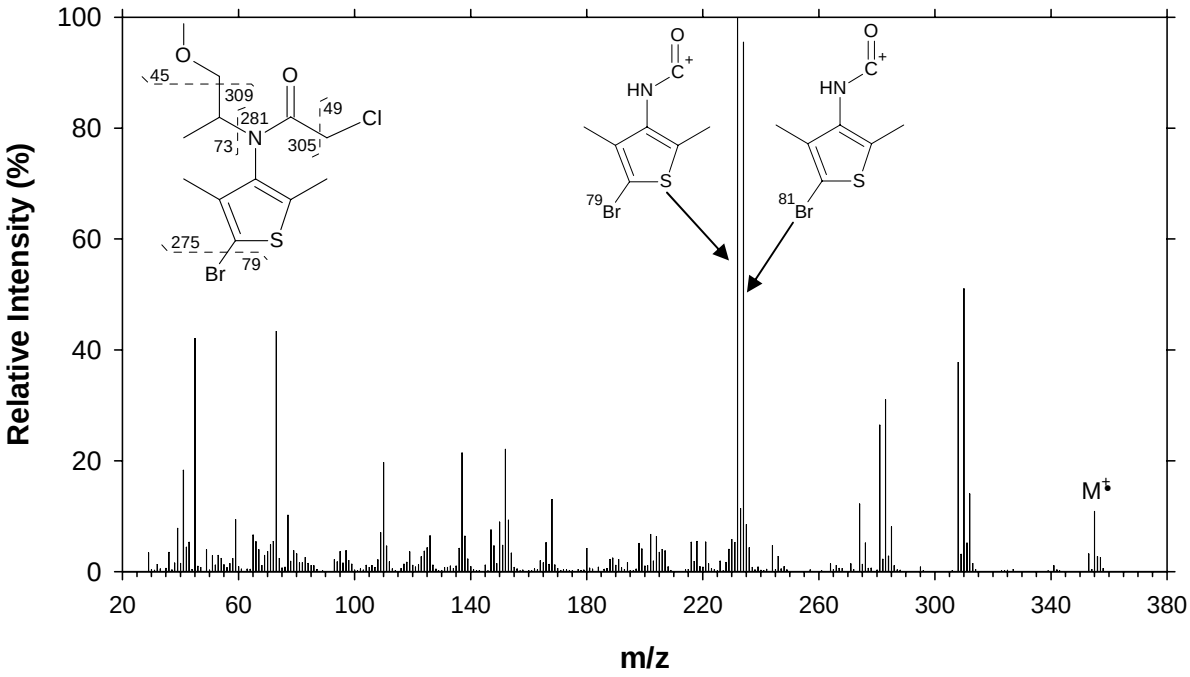

Figure S2. Mass spectrum of bromodimethenamid with identification of selected fragments.

Table S2. ^{1}H NMR data for dimethenamid, chlorodimethenamid and bromodimethenamid.

	Dimethenamid (R = H)			Chlorodimethenamid (R = Cl)			Bromodimethenamid (R = Br)		
Assignment	δ *(ppm)* [a]	*Multiplicity* [b]	*Integration*	δ *(ppm)* [a]	*Multiplicity*	*Integration*	δ *(ppm)* [a]	*Multiplicity*	*Integration*
a	1.11	d	3H	1.11	d	3H	1.15	d	3H
b	2.07	s	3H	2.01	s	3H	2.02	s	3H
c	2.35	s	3H	2.30	s	3H	2.32	s	3H
d	3.29	d	3H	3.29	d	3H	3.27	d	3H
e	3.39	d	2H	3.39	d	2H	3.30	d	2H
f	3.54	m	1H	3.54	m	1H	3.52	m	1H
g	3.67	s	2H	3.67	s	2H	3.68	s	2H
h	6.82	s	1H	No Signal			No Signal		

[a] All analytes have a chiral carbon center (denoted with an asterisk in Figure S3) and exist as a mixture of enantiomers. Reported chemical shifts are average values among enantiomers in $CDCl_3$.

[b] s = singlet, d = doublet, m = multiplet.

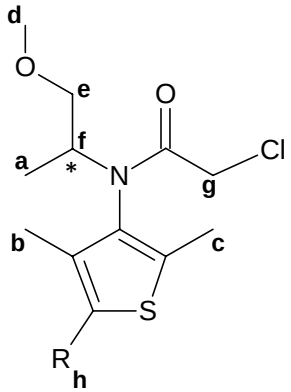

Figure S3. Atom labeling for ^{1}H NMR assignments of dimethenamid (R = H), chlorodimethenamid (R = Cl) and bromodimethenamid (R = Br) listed in Table S2. * Denotes chiral carbon center.

6. Example time courses

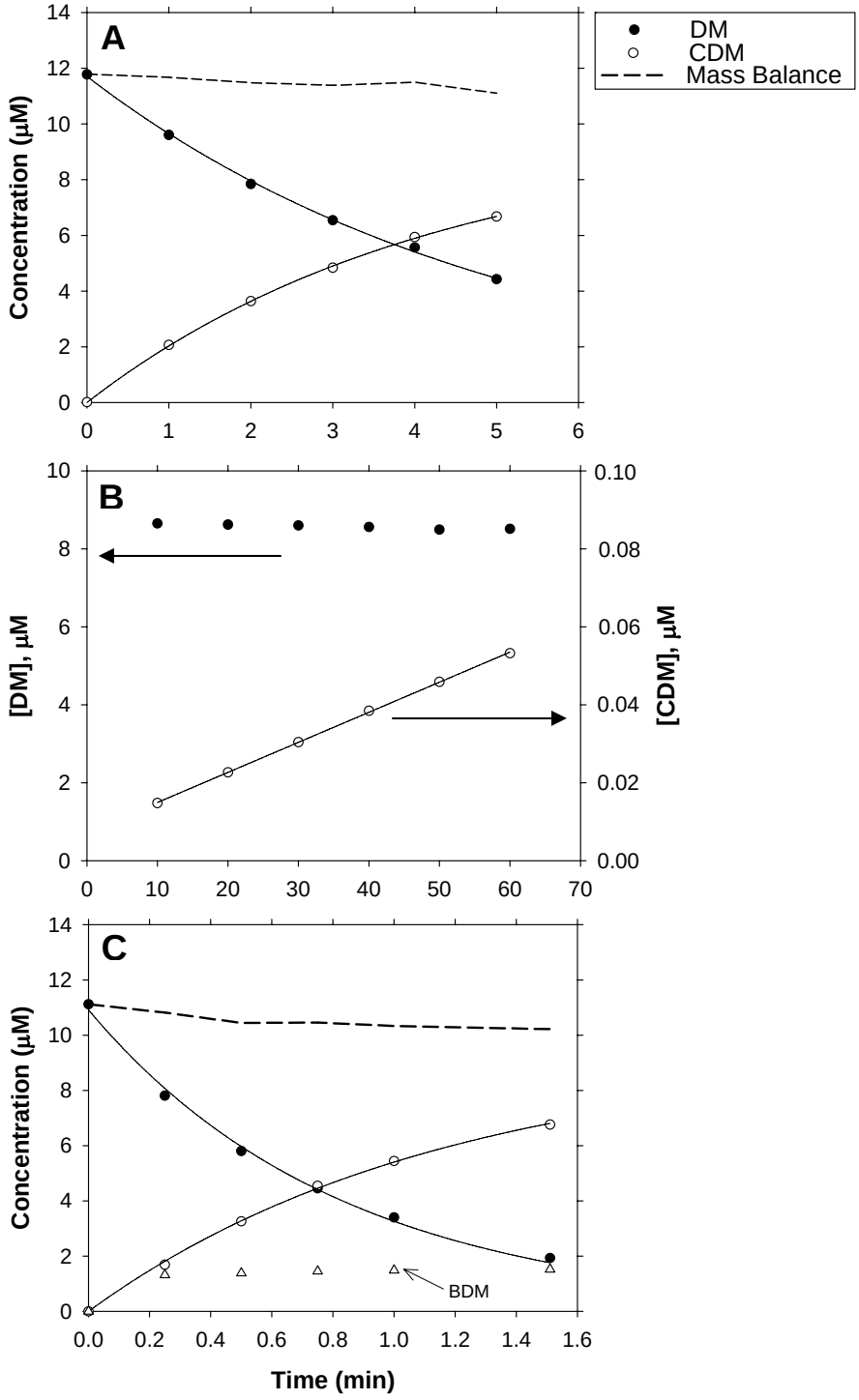

Figure S4. Time courses for the reaction of DM with FAC in solutions containing (**A**) no chloride amendment at pH 6.3; (**B**) no chloride amendment at pH 9.4; and (**C**) 30 mM NaCl at pH 6.3. Formation of bromodimethenamid (BDM) is the result of trace bromide contamination in NaCl; mass balance includes [BDM]. Lines denote model fits to the data according to Equations 4 – 6 (see main text). Conditions: $[DM]_o$ = 1.1 x 10^{-5} M, $[FAC]_o$ = 6 x 10^{-4} M, [phosphate or borate buffer] = 0.01 M, $[NaNO_3]$ + [NaCl] = 0.1 M, T = 25.0 ± 0.1°C.

7. Derivation of Equation 5: Reaction kinetics in the presence of trace bromide

DM can react with Cl_2, Cl_2O and HOCl to give CDM. Accordingly, the rate of CDM formation can be written as:

$$\frac{d[CDM]}{dt} = (k_{Cl2}[Cl_2] + k_{Cl2O}[Cl_2O] + k_{HOCl}[HOCl])[DM] \quad [S1]$$

In reactors to which NaCl has been added, low levels of bromide are present and serve as a reductant of FAC. In these reactors, $[FAC]_o >> [DM]_o + [Br^-]_o$, and therefore pseudo-first-order conditions are maintained. Thus, Equation S1 can be simplified to:

$$\frac{d[CDM]}{dt} = k_{obs}[DM] \quad [S2]$$

where $k_{obs} = k_{Cl2}[Cl_2] + k_{Cl2O}[Cl_2O] + k_{HOCl}[HOCl]$.

In the presence of FAC and trace bromide, DM can undergo both chlorination and bromination reactions to yield chlorodimethenamid (CDM) and bromodimethenamid (BDM), respectively. The mass balance for DM can be expressed as:

$$[DM]_o = [DM] + [CDM] + [BDM] \quad [S3]$$

Using Equation S3 to substitute for [DM] in Equation S2 yields:

$$\frac{d[CDM]}{dt} = k_{obs}([DM]_o - [CDM] - [BDM]) \quad [S4]$$

In NaCl-fortified reactors, time course data (**Figure S4C**) suggest bromination reactions of DM are fast relative to chlorination reactions and that bromide is the limiting reagent for the formation of BDM (*i.e.*, $[Br^-]_o < [DM]_o$). Under these conditions, *ca.* quantitative conversion of $[Br^-]_o$ to [BDM] occurs by the second time point (**Figure S4C**), after which $[BDM] \approx [Br^-]_o$. Making this substitution for BDM in Equation S4 gives:

$$\frac{d[CDM]}{dt} \cong k_{obs}([DM]_o - [CDM] - [Br^-]_o) \quad [S5]$$

Rearranging Equation S5 and combining constants such that $C = [DM]_o - [Br^-]_o$ yields:

$$\frac{d[CDM]}{C-[CDM]} = k_{obs}dt \quad [S6]$$

Integrating Equation S6 gives:

$$ln\left(\frac{C-[CDM]}{C-[CDM]_o}\right) = -k_{obs}t \quad [S7]$$

Noting that $[CDM]_o = 0$ and solving for [CDM] yields:

$$[CDM] = C\{1-\exp(-k_{obs}t)\} \quad [S8]$$

Recalling that $C = [DM]_o - [Br^-]_o$ gives the final result (Equation 5 from the main text):

$$[CDM] = ([DM]_o - [Br^-]_o)\{1-\exp(-k_{obs}t)\} \quad [S9]$$

8. Reaction order in [DM]

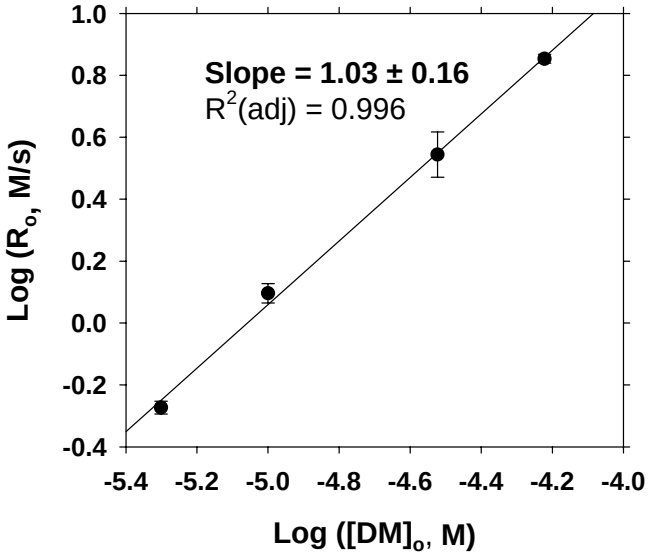

Figure S5. Log-log plot of initial CDM formation rate (R_o) as a function of initial DM concentration ($[DM]_o$ = 5.0 x 10^{-6} M to 6.0 x 10^{-5} M). Uniform conditions: pH 6.4, [phosphate buffer] = 0.010 M, $[FAC]_o$ = 6 x 10^{-4} M, $[NaNO_3]$ = 0.10 M, no NaCl amendment. Error estimates denote 95% confidence intervals. R_o values were calculated as the slope of [CDM] versus time regressions for conditions under which the extent of reaction was < 10% of $[DM]_o$.

9. Reaction order in [FAC]

The experimentally determined reaction orders in [FAC] (n) and corresponding solution conditions are compiled in **Table S3**. Also shown is the reaction order range calculated (n_{calc}) assuming an average of the reactivities of individual chlorinating agents, weighted by their individual reaction order in [FAC] (2, 1 and 1 for Cl_2O, Cl_2 and HOCl, respectively):

$$n_{calc} = \frac{2k_{Cl2O}[Cl_2O] + k_{Cl2}[Cl_2] + k_{HOCl}[HOCl]}{k_{Cl2O}[Cl_2O] + k_{Cl2}[Cl_2] + k_{HOCl}[HOCl]} \quad [S10]$$

For the limiting case of $k_{Cl2O}[Cl_2O] >> k_{Cl2}[Cl_2] + k_{HOCl}[HOCl]$, $n_{calc} = 2$. Conversely, when the reactivity of either Cl_2 or HOCl (or their sum) predominates, then $n_{calc} = 1$. As shown in **Table S3**, n values are generally in close agreement with n_{calc} values determined via Equation S10. A derivation of Equation S10 begins on the next page.

Table S3. Experimentally measured (n) and calculated (n_{calc}) reaction orders in [FAC] of DM chlorination as a function of pH, [Cl^-], and [FAC].[a]

pH	*[Cl⁻], mM*	*[FAC] range*	*n*	n_{calc} *range* [b]
6.5	30	$2.0 \times 10^{-4} – 9.9 \times 10^{-4}$	1.10 ± 0.13	1.14 – 1.45
6.9	30	$9.8 \times 10^{-5} – 1.0 \times 10^{-3}$	1.26 ± 0.10	1.15 – 1.64
7.3	3.0	$9.8 \times 10^{-5} – 8.1 \times 10^{-4}$	1.29 ± 0.21	1.63 – 1.93
7.7	3.0	$3.0 \times 10^{-4} – 1.5 \times 10^{-3}$	1.56 ± 0.19	1.82 – 1.96
7.0	0.3 [c]	$1.5 \times 10^{-5} – 1.4 \times 10^{-4}$	1.46 ± 0.19	1.37 – 1.84
7.2	0.3 [c]	$3.5 \times 10^{-5} – 2.1 \times 10^{-4}$	1.60 ± 0.18	1.55 – 1.88
7.3	0.3 [c]	$2.0 \times 10^{-4} – 1.1 \times 10^{-3}$	1.78 ± 0.22	1.87 – 1.97
7.6	0.3 [c]	$3.5 \times 10^{-5} – 2.1 \times 10^{-4}$	1.50 ± 0.22	1.46 – 1.84

[a] Error ranges denote 95% confidence intervals. $[DM]_o = 1.0 \times 10^{-5}$ M; [NaCl] + [$NaNO_3$] = 0.1 M.
[b] Calculated via Equation S10 using the minimum and maximum experimental [FAC] values; equilibrium concentrations of FAC components calculated via Equations 1 – 3 in the main text. Employed rate constants (units: M^{-1} s^{-1}): $k_{Cl2O} = (1.37 \pm 0.17) \times 10^6$, $k_{Cl2} = (1.21 \pm 0.06) \times 10^6$, and $k_{HOCl} = 0.18 \pm 0.10$; see Section 15 below for details of how rate constants were calculated.
[c] No added chloride

Derivation of Equation S10.

The rate constant for the reaction of DM in solutions of FAC can be expressed as:

$$k_{obs} = k_{Cl2O}[Cl_2O] + k_{Cl2}[Cl_2] + k_{HOCl}[HOCl] \quad [S11]$$

Using Equations 2 and 3 to substitute for [Cl_2] and [Cl_2O], respectively, yields:

$$k_{obs} = k_{Cl2O}K_3[HOCl]^2 + k_{Cl2}K_2[Cl^-][H^+][HOCl] + k_{HOCl}[HOCl] \quad [S12]$$

Factoring out [HOCl] gives:

$$k_{obs} = [HOCl](k_{Cl2O}K_3[HOCl] + k_{Cl2}K_2[Cl^-][H^+] + k_{HOCl}) \quad [S13]$$

Applying a common logarithmic function to Equation S13 yields:

$$\log k_{obs} = log[HOCl] + log(k_{Cl2O}K_3[HOCl] + k_{Cl2}K_2[Cl^-][H^+] + k_{HOCl}) \quad [S14]$$

Grouping the constants in Equation S14 gives:

$$\log k_{obs} = log[HOCl] + log(C_1[HOCl] + C_2) \quad [S15]$$

where $C_1 = k_{Cl2O}K_3$ and $C_2 = k_{Cl2}K_2[Cl^-][H^+] + k_{HOCl}$

As shown in Equation 7, the reaction order in [FAC] (n_{calc}) is calculated as the slope of a linear regression of log k_{obs} versus log [FAC]. Stated more formally:

$$n_{calc} = \frac{d(\log k_{obs})}{d(\log [FAC])} \quad [S16]$$

Recall that [FAC] ≈ [HOCl] + [OCl^-]. Substituting for [OCl^-] from Equation 1 gives:

$$[FAC] = [HOCl] + [HOCl]K_1/[H^+] = [HOCl](1 + K_1/[H^+]) \quad [S17]$$

Taking logarithms gives:

$$\log[FAC] = \log[HOCl] + \log(1 + K_1/[H^+]) \quad [S18]$$

Differentiating Equation S18 yields:

$$\frac{d(\log [FAC])}{d(\log [HOCl])} = 1 \quad [S19]$$

Equivalently:

$$d(\log [FAC]) = d(\log [HOCl]) \quad [S20]$$

Substituting Equation S20 into Equation S16 gives:

$$n_{calc} = \frac{d(\log k_{obs})}{d(\log [HOCl])} \quad [S21]$$

Applying the derivative shown in Equation S21 to Equation S15 yields:

$$n_{calc} = \frac{d(\log k_{obs})}{d(\log [HOCl])} = 1 + \frac{d}{d(\log [HOCl])}(log(C_1[HOCl] + C_2) \quad [S22]$$

Evaluating the right-hand side of Equation S22 requires application of the chain rule:

$$\frac{d}{d(\log [HOCl])}\left(log(C_1[HOCl] + C_2)\right) = \frac{d[HOCl]}{d(\log [HOCl])}\frac{d}{d[HOCl]}\left(log(C_1[HOCl] + C_2)\right) \quad [S23a]$$

$$= [HOCl]\left(\frac{C_1}{C_1[HOCl] + C_2}\right) \quad [S23b]$$

Substituting Equation S23b into Equation S22 gives:

$$n_{calc} = 1 + [HOCl]\left(\frac{C_1}{C_1[HOCl] + C_2}\right) \quad [S24]$$

Rearranging Equation S24 yields:

$$n_{calc} = \frac{2C_1[HOCl] + C_2}{C_1[HOCl] + C_2} \quad [S25]$$

Multiplying the numerator and denominator of Equation S25 by [HOCl] gives:

$$n_{calc} = \frac{2C_1[HOCl]^2 + C_2[HOCl]}{C_1[HOCl]^2 + C_2[HOCl]} \quad [S26]$$

Replacing C_1 and C_2 with their original values gives:

$$n_{calc} = \frac{2K_3k_{Cl2O}[HOCl]^2 + k_{Cl2}K_2[Cl^-][H^+][HOCl] + k_{HOCl}[HOCl]}{K_3k_{Cl2O}[HOCl]^2 + k_{Cl2}K_2[Cl^-][H^+][HOCl] + k_{HOCl}[HOCl]} \quad [S27]$$

Substituting $[Cl_2]$ and $[Cl_2O]$ from Equations 2 and 3, respectively, into Equation S27 gives the desired result:

$$n_{calc} = \frac{2k_{Cl2O}[Cl_2O]+k_{Cl2}[Cl_2]+ k_{HOCl}[HOCl]}{k_{Cl2O}[Cl_2O]+k_{Cl2}[Cl_2]+ k_{HOCl}[HOCl]} \quad [S10]$$

10. Exploration of Cl_2O formation as a potentially rate-limiting step

Some previous researchers have found Cl_2O formation to be rate-limiting during reactions with organic (*S2-S4*) and inorganic (*S5*) reductants. In such a case, we would expect Cl_2O to be rapidly depleted through reaction with DM. This would lead to reaction rates that slowed over time. In the current work, excellent linear fits of ln([DM]) versus time (R^2 typically > 0.99) were obtained, even though $[DM]_o$ was greatly in excess of computed concentrations of Cl_2O. Moreover, reactions were first-order in [DM] for all examined $[DM]_o$ in solution conditions such that reactions with Cl_2O account for 95% of the total rate of CDM formation (**Figure S5**). The observed first-order dependence of reaction rates on [DM] implies that re-establishment of Cl_2O equilibrium on dilution of FAC stock solution, as well as regeneration of Cl_2O from HOCl following Cl_2O reaction with DM, were both fast relative to the rate of Cl_2O reaction with DM.

11. Stoichiometry data

To explore whether the second-order dependence of DM reaction rates on [HOCl] might stem from a termolecular reaction involving two equivalents of HOCl per mole of DM, stoichiometry experiments were performed in which changes in the concentrations of DM and FAC were simultaneously monitored. Experiments were conducted using equal initial concentrations (0.10 mM) of both DM and FAC in solutions with initial volumes of 40 mL. All other conditions and sampling protocols were identical to those described in the Experimental Section of the main text. Samples were simultaneously obtained for FAC analysis (2.00 mL aliquot) and DM extraction into toluene (0.80 mL aliquot). FAC concentrations were determined as described in the main text immediately after each sample was obtained.

Shown in **Figure S6** are the results from two stoichiometry experiments performed under different solution conditions. In **Figure S6A**, the solution conditions were pH 4.1 and $[Cl^-] = 0.3$ mM. In **Figure S6B**, the solution conditions were pH 6.9 and $[Cl^-] = 30$ mM. In both cases, a 1:1 stoichiometry between DM and FAC is indicated by the slopes of the $-\Delta[DM]$ versus $-\Delta[FAC]$ plots. These results do not support a termolecular reaction, for which a 1:2 stoichiometry between DM and FAC might be expected. The results are, however, consistent with theoretical stoichiometries if Cl_2O, Cl_2 or HOCl were the reactive chlorinating species, as illustrated below.

In the case of Cl_2O as the chlorinating agent of DM, the products are CDM, H^+ (lost from DM) and OCl^- (the leaving group of Cl_2O):

$$Cl_2O + DM \rightarrow CDM + H^+ + OCl^- \qquad [S28]$$

Recall the dissociation equilibrium for HOCl:

$$H^+ + OCl^- \leftrightarrow HOCl \qquad [S29]$$

and the dehydration reaction of HOCl forming Cl_2O:

$$2\ HOCl \leftrightarrow Cl_2O + H_2O \qquad [S30]$$

Summing Equations S28 – S30 yields:

$$HOCl + DM \rightarrow CDM + H_2O \qquad [S31]$$

which clearly indicates the 1:1 theoretical stoichiometry between DM and HOCl, and therefore a 1:1 stoichiometry between DM and FAC (noting that [FAC] ≈ [HOCl] + [OCl^-]) with Cl_2O (or HOCl) functioning as the active chlorinating agent.

Similarly, in the case of Cl_2 reacting with DM, the products are CDM, H^+, and Cl^- (the nucleofuge of Cl_2):

$$Cl_2 + DM \rightarrow CDM + H^+ + Cl^- \qquad [S32]$$

The formation of aqueous Cl_2 from HOCl can be expressed as:

$$HOCl + H^+ + Cl^- \leftrightarrow Cl_2 + H_2O \qquad [S33]$$

Combining Equations S32 and S33 gives Equation S31, and thus a 1:1 stoichiometry between DM and FAC when Cl_2 is the chlorinating agent.

In summary, all chlorinating agents considered above (*i.e.*, Cl_2O, Cl_2 and HOCl) have a theoretical stoichiometry of 1:1 for reactions with DM. Thus, although the stoichiometry data are consistent with all chlorinating agents under consideration, the stoichiometry data do not allow for delineation of the relative contributions of these species during reactions with DM.

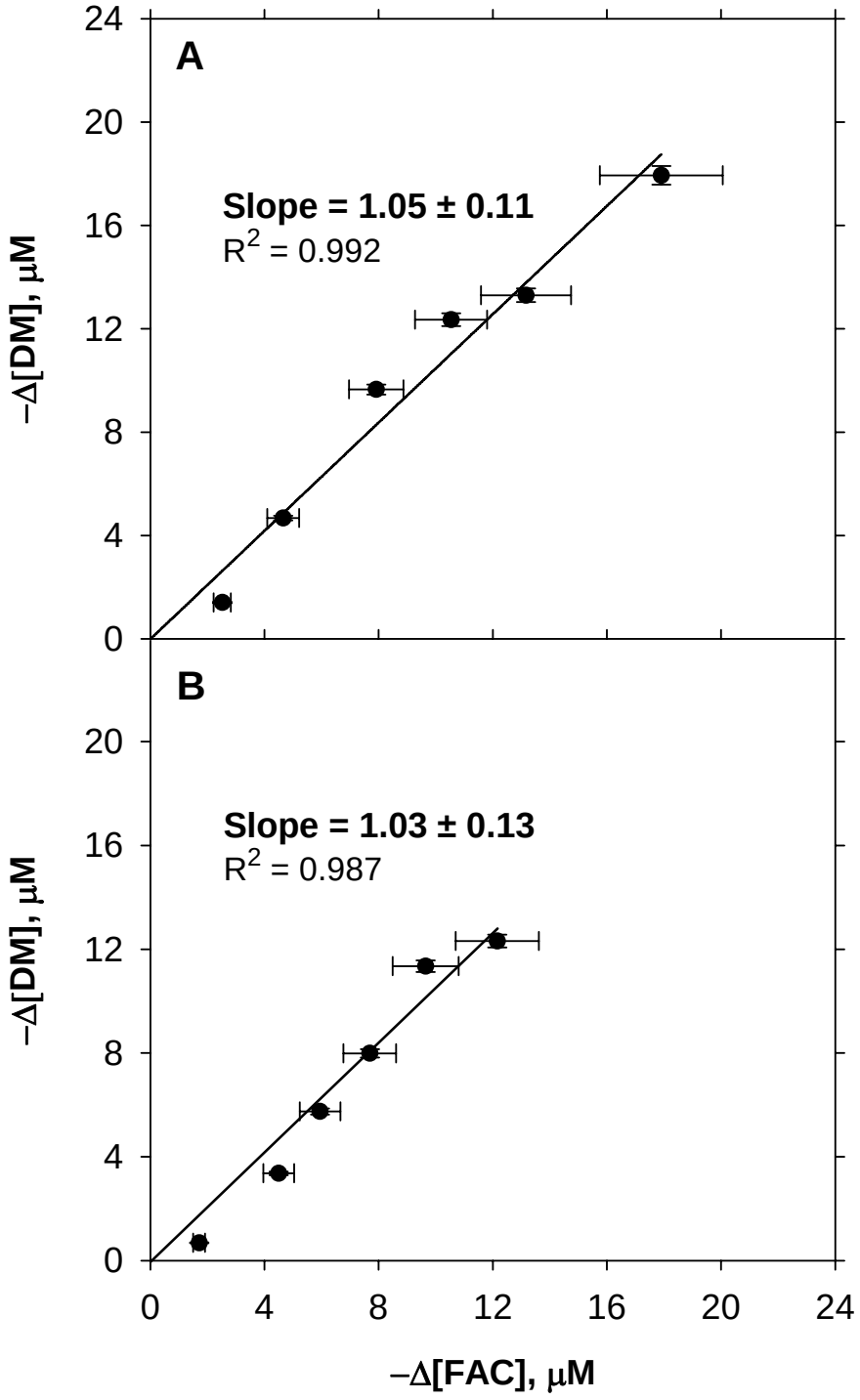

Figure S6. Stoichiometry experiments for the reaction of DM with FAC at (**A**) pH 4.1, $[Cl^-]$ = 0.3 mM and (**B**) pH 6.9, $[Cl^-]$ = 30 mM. Other conditions: $[FAC]_o = [DM]_o$ = 100 μM, [NaCl] + $[NaNO_3]$ = 0.1 M, [acetate or phosphate buffer] = 0.01 M, T = 25.0 ± 0.1°C. Slope values were determined from linear regressions forced through the origin; error estimates denote 95% confidence intervals.

12. Exploration of acid catalysis effects

Previous researchers (*S6-S9*) have hypothesized that a protonated HOCl species (H_2OCl^+) best explains the enhanced reactivity of FAC at low pH. To explore the possible role of acid catalysis during the transformation of DM, experimental results were analyzed as a function of chloride concentration at five pH values spanning pH 5.2 – 6.4. The results are shown in **Figure S7**. Linear regressions of the data at each pH level were performed to afford extrapolation of k_{obs} to $[Cl^-] = 0$ (*i.e.,* calculation of y-intercepts). As $[Cl^-] \rightarrow 0$, the data converge to a single k_{obs} value, $(3.6 \pm 1.2) \times 10^{-3}$ s^{-1}. As such, no acid catalysis is indicated, suggesting that Cl_2 (rather than H_2OCl^+) is responsible for the rate enhancement with decreasing pH. This finding is consistent with a recent report (*S10*) employing Raman spectroscopy, which indicated that Cl_2 (rather than H_2OCl^+) is the reactive species in nominally "chloride-free" FAC solutions at low pH.

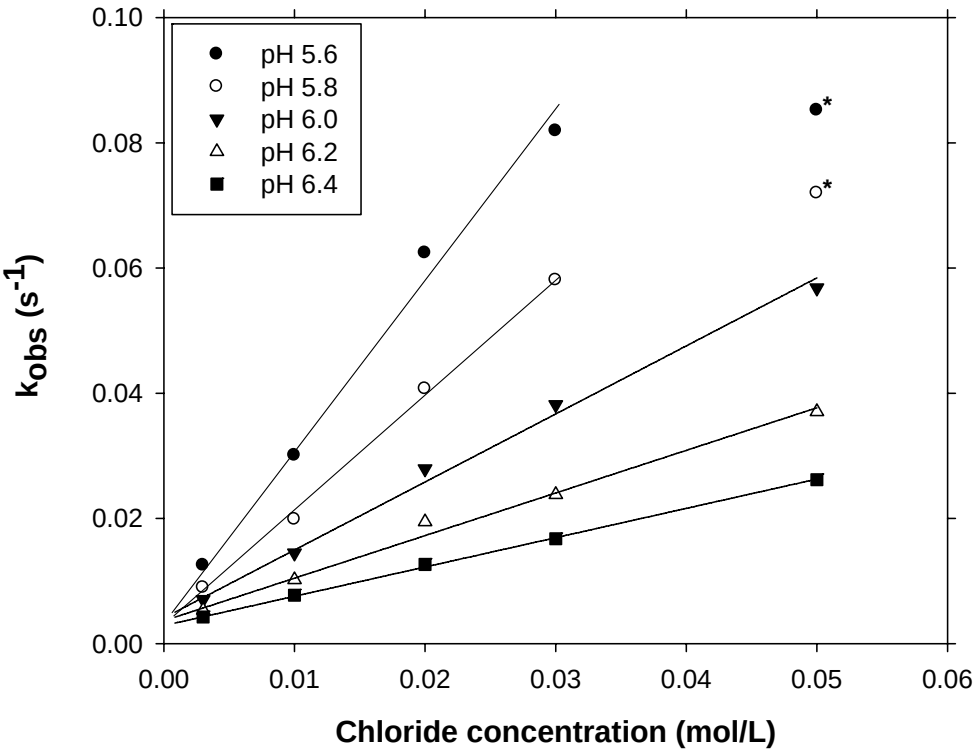

Figure S7. Rate constants for the reaction of DM with FAC as a function of chloride concentration at five pH values from k_{obs} data shown in Figure S8. When data were not available at a desired pH value, k_{obs} values were interpolated; data points used for interpolation were typically within ± 0.1 pH unit of the target values specified in the legend. Uniform conditions: $[DM]_o = 1.0 \times 10^{-5}$ M, $[FAC]_o = 6 \times 10^{-4}$ M, acetate (pH < 6.0) or phosphate (pH ≥ 6.0) [buffer] = 0.010 M, [NaCl] + [$NaNO_3$] = 0.1 M. Data points marked with an asterisk (*) are approaching the maximum k_{obs} value (~ 0.1 s^{-1}) measurable by our method and were excluded from linear regressions.

13. Calculation of chloride concentrations in reactors with no NaCl amendment

The rate constant (k_{obs}) for the reaction of DM with FAC species to give CDM can be expressed as:

$$k_{obs} = k_{Cl2}[Cl_2] + k_{Cl2O}[Cl_2O] + k_{HOCl}[HOCl] \quad \text{[S11]}$$

For the series of reactions in which [Cl^-] was varied (**Figure S7**), it is useful to rewrite Equation S11 noting that [Cl_2] = K_2[HOCl][H^+][Cl^-] (see Equation 2 in main text):

$$k_{obs} = k_{Cl2}K_2[HOCl][H^+][Cl^-] + b \quad \text{[S34]}$$

where $b = k_{Cl2O}$[Cl_2O] + k_{HOCl}[HOCl]. Note that b is not a function of [Cl^-] (at constant ionic strength). At constant pH, ionic strength and [FAC], Equation S34 simplifies further to:

$$k_{obs} = a[Cl^-] + b \quad \text{[S35]}$$

where $a = k_{Cl2}K_2$[HOCl][H^+] and both a and b are constants. Values of a and b were determined by regressing k_{obs} values measured at pH 6.0 versus [Cl^-] in NaCl-fortified reactors (data shown in **Figure S7**). Once a and b were determined, background [Cl^-] could be estimated using k_{obs} values obtained at pH 6.0 in nominally chloride-free reactors as:

$$[Cl^-] = \frac{k_{obs} - b}{a} \quad \text{[S36]}$$

Of the five regressions shown in **Figure S7**, the regression obtained with the pH 6.0 data gave the most precise estimate of [Cl^-] (0.3 ± 0.1 mM) when the k_{obs} value measured at pH 6.0 with no added chloride ((3.8 ± 0.2) x 10^{-3} s^{-1}) was substituted into Equation S36. Estimates of [Cl^-] obtained using data at the other pH values shown in **Figure S7** were not different (at the 95% confidence levels) from the value obtained at pH 6.0. The [Cl^-] calculated above is in agreement with post-reaction ion chromatography measurements, which found [Cl^-] ≤ 0.9 mM.

14. Comprehensive data for DM reactions versus pH

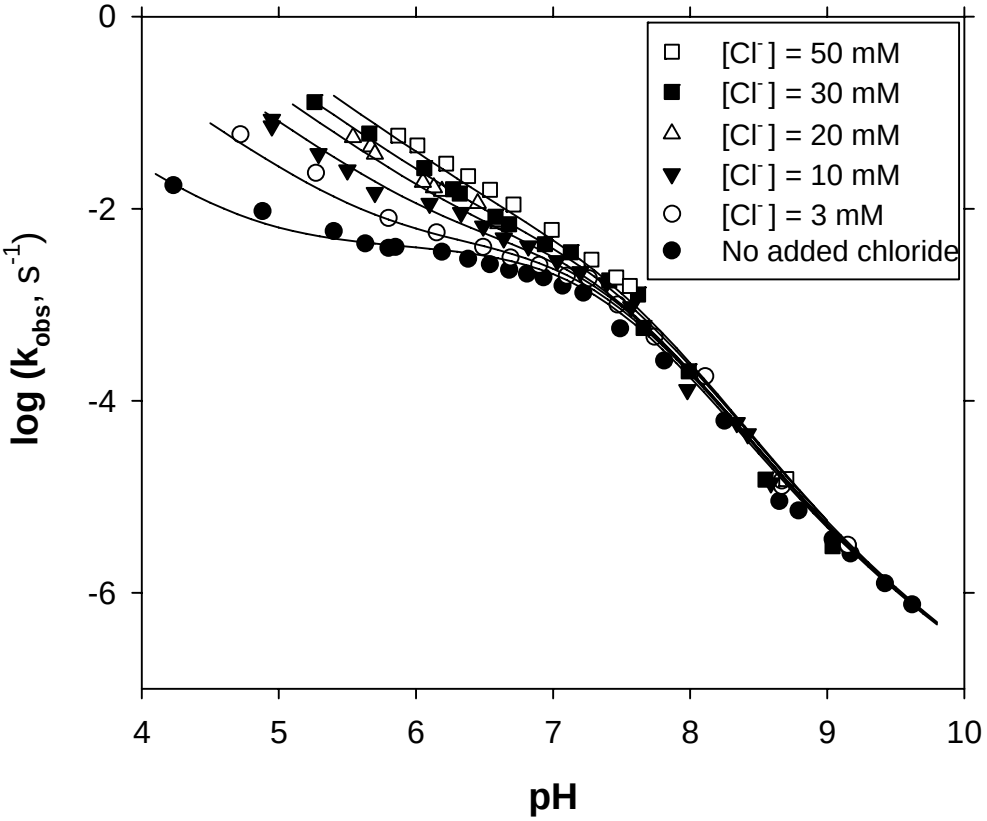

Figure S8. Rate constants (log k_{obs}) for the formation of CDM from reactions of DM with FAC as a function of pH at six chloride levels. Uniform conditions: $[FAC]_o$ = 6 x 10^{-4} M, [NaCl] + [$NaNO_3$] = 0.1 M, [acetate, phosphate or borate buffer] = 0.010 M, T = 25.0 ± 0.1°C. Solid lines denote model fits of the form: $k_{obs} = k_{Cl2O}[Cl_2O] + k_{Cl2}[Cl_2] + k_{HOCl}[HOCl]$.

15. Determination of second-order rate constants

Concentrations of FAC species in each experimental system were calculated using the equilibrium constants listed for Equations 1 – 3 in the main text, corrected for ionic strength and temperature. Speciation data and the corresponding k_{obs} values were analyzed using the program *Scientist*® v3.0 (MicroMath®) to determine second-order rate constants for individual chlorinating agents assuming the following reactivity model:

$$k_{obs} = k_{Cl2}[Cl_2] + k_{Cl2O}[Cl_2O] + k_{HOCl}[HOCl] \quad [S11]$$

Each second-order rate constant was fit sequentially as described below. Best fits to Equation S11 were obtained when all three FAC species were considered. In all cases, inclusion of a term for OCl^- into Equation S11 resulted in either no improvement or poorer fits to the data.

To obtain a precise estimate of k_{Cl2}, data from experiments containing a NaCl fortification (3 mM – 50 mM) at pH < 7.0 were modeled, and the following rate constants were obtained (units are M^{-1} s^{-1} and uncertainty estimates denote 95% confidence intervals for all rate constants below): k_{Cl2} = (1.21 ± 0.06) x 10^6 and k_{Cl2O} = (1.9 ± 0.7) x 10^6 (k_{HOCl} was fixed at 0). To improve the estimate of k_{Cl2O}, the subset of data containing no chloride fortification at pH < 8.0 were modeled assuming a fixed value of k_{Cl2} = 1.21 x 10^6 and k_{HOCl} = 0. Under these conditions, the relative importance of Cl_2O is expected to increase due to the absence of added chloride. The resulting k_{Cl2O} was (1.37 ± 0.17) x 10^6. Finally, to obtain a precise estimate of k_{HOCl}, only data obtained at pH ≥ 8.8 with no chloride fortification were considered. Under these conditions, the contribution of Cl_2 is negligible and k_{obs} can be modeled considering only Cl_2O and HOCl. Assuming a fixed value of k_{Cl2O} = 1.37 x 10^6, k_{HOCl} was calculated as 0.18 ± 0.10. Recalculation of k_{Cl2} and k_{Cl2O} using the entire data set and assuming a fixed value of 0.18 for k_{HOCl} did not further improve model fits.

The second-order rate constants reported above are only as robust as the corresponding equilibrium constants used to calculate concentrations of individual FAC species. In particular, uncertainties associated with reported values of K_3 have been discussed (*S11*). Roth (*S12*) calculated K_3 as 8.70×10^{-3} M^{-1} at 19°C from H_2O/CCl_4 partitioning data. Reinhard *et al*. (*S11*) employed calorimetric titrations and found that K_3 was < 1 M^{-1}. The calorimetry data of Reinhard *et al*. (*S11*) did not afford a precise calculation of K_3, but rather only an upper limit. The authors (*S11*) concluded that solution calorimetry was unsuitable for an accurate determination of K_3 due to the small reaction enthalpy of Cl_2O hydrolysis (Equation 3). As the K_3 value reported by Roth (*S12*) is the more robust estimate, it was used for all pertinent calculations in the current work (after adjustment to 25°C; see Equation 3 and discussion immediately following).

Uncertainties in K_3 will certainly affect calculated values of $[Cl_2O]$ and, hence, k_{Cl2O}. We note, however, that uncertainties in K_3 do <u>not</u> affect the magnitude of the contribution made by Cl_2O to the rate of DM reaction, expressed in Figure 5 as the composite term $k_{Cl2O}[Cl_2O]$. It is, after all, this composite term that is directly reflected by k_{obs} measurements; estimates of K_3 simply dictate how this is apportioned into $[Cl_2O]$ versus k_{Cl2O}. If new measurements of the stability constant K_3 for Cl_2O were to emerge, any revisions to computed values of $[Cl_2O]$ in our experiments would be exactly compensated by adjustments to k_{Cl2O} such that the composite term (and, hence, the relative importance of Cl_2O) would remain unaltered.

When Cl_2O controls the chlorination rate of DM, Equation S11 reduces to:

$$k_{obs} = k_{Cl2O}[Cl_2O] \qquad [S37]$$

As indicated by Equation S37, uncertainties in the composite term $k_{Cl2O}[Cl_2O]$ are controlled solely by the precision of measured k_{obs} values.

16. Relative importance of Cl_2O versus HOCl for other compounds

Cl_2O will influence reaction rates of FAC solutions to a greater extent than HOCl when $k_{Cl2O}[Cl_2O] > k_{HOCl}[HOCl]$, or equivalently, when $k_{Cl2O}/k_{HOCl} > [HOCl]/[Cl_2O]$. Assuming a typical DW chlorination level ([HOCl] = 2.1 x 10^{-5} M), $[HOCl]/[Cl_2O] \approx 5 \times 10^6$. Thus, when $k_{Cl2O}/k_{HOCl} > ca.\ 5 \times 10^6$, Cl_2O will be a more facile oxidant than HOCl. For DM, the relative reactivity of Cl_2O and HOCl is given by $k_{Cl2O}/k_{HOCl} = 7.6 \times 10^6$ (25°C). If k_{HOCl} for other compounds were to exceed 1300 $M^{-1}\ s^{-1}$ and the same relative reactivity of Cl_2O and HOCl were to pertain, k_{Cl2O} would approach $10^{10}\ M^{-1}\ s^{-1}$ and, hence, diffusion limitations would be reached. Past this point, the greater inherent reactivity of Cl_2O could no longer compensate for its lower concentration, and the relative importance of Cl_2O would diminish.

Caution must be exercised, however, when invoking values of k_{HOCl} previously reported in the literature. In many instances, attempts to delineate contributions from reactive FAC species other than HOCl have not been made, and k_{HOCl} is assumed equal to:

$$k_{HOCl} = \frac{k_{obs}}{[HOCl]} \qquad [S38]$$

Only when HOCl accounts for ~100% of the total FAC reactivity would Equation S38 provide accurate estimates of k_{HOCl}. As illustrated in **Figure 5**, in the case of DM reaction with FAC, such conditions are unlikely to be encountered during DW or WW treatment. They may be even less common in the laboratory experiments from which k_{HOCl} values reported in the literature are derived. Depending on the specific [FAC], pH, and chloride concentrations employed, values of k_{HOCl} computed according to Equation S38 may be substantially in error. For example, in our own experiments in the absence of added chloride at pH 7.0 and [FAC] = 6 x 10^{-4} M, applying Equation S38 would have resulted in a computed value for k_{HOCl} of 4.0 $M^{-1}\ s^{-1}$, a factor of 22 larger than our measured value. At an FAC content of 6 x 10^{-3} M and an equimolar concentration

of chloride (conditions that are not atypical of laboratory studies), the error in values of k_{HOCl} computed in this manner (with k_{obs} calculated from Equation S11) would increase to a factor of 55 at pH 7 and 165 at pH 5.

17. Literature Cited

(S1) Hladik, M. L.; Roberts, A. L.; Bouwer, E. J. Removal of neutral chloroacetamide herbicide degradates during simulated unit processes for drinking water treatment. *Water Res.* **2005,** *39*, 5033-5044.

(S2) Israel, G. C.; Martin, J. K.; Soper, F. G. The kinetics of chlorohydrin formation. Part I. The reaction between hypochlorous acid and allyl alcohol in aqueous solution. *J. Chem. Soc.* **1950**, 1282-1285.

(S3) Craw, D. A.; Israel, G. C. The kinetics of chlorohydrin formation. Part III. The reaction between hypochlorous acid and crotonic acid at constant pH. *J. Chem. Soc.* **1952,** 550-553.

(S4) Swain, C. G.; Crist, D. R. Mechanisms of chlorination by hypochlorous acid. The last of chlorinium ion, Cl^+. *J. Am. Chem. Soc.* **1972,** *94*, 3195-3200.

(S5) Beach, M. W.; Margerum, D. W. Kinetics of oxidation of tetracyanonickelate(II) by chlorine monoxide, chlorine, and hypochlorous acid and kinetics of chlorine monoxide formation. *Inorg. Chem.* **1990,** *29*, 1225-1232.

(S6) Rebenne, L. M.; Gonzalez, A. G.; Olson, T. M. Aqueous chlorination kinetics and mechanism of substituted dihydroxybenzenes. *Environ. Sci. Technol.* **1996,** *30*, 2235-2242.

(S7) Gallard, H.; Von Gunten, U. Chlorination of phenols: Kinetics and formation of chloroform. *Environ. Sci. Technol.* **2002,** *36*, 884-890.

(S8) Gallard, H.; Leclercq, A.; Croué, J. P. Chlorination of bisphenol A: Kinetics and by-products formation. *Chemosphere* **2004,** *56*, 465-473.

(S9) Deborde, M.; Rabouan, S.; Gallard, H.; Legube, B. Aqueous chlorination kinetics of some endocrine disruptors. *Environ. Sci. Technol.* **2004,** *38*, 5577-5583.

(S10) Cherney, D. P.; Duirk, S. E.; Tarr, J. C.; Collette, T. W. Monitoring the speciation of aqueous free chlorine from pH 1 to 12 with Raman spectroscopy to determine the identity of the potent low-pH oxidant. *Appl. Spectrosc.* **2006,** *60*, 764-772.

(S11) Reinhard, M.; Redden, G. D.; Voudrias, E. A. The hydrolysis constants of chlorine monoxide and bromine chloride in water*; In* Jolley, R. L., *et al*. (Eds.); *Water Chlorination: Environmental Impact and Health Effects*; Ann Arbor Science: Ann Arbor, MI: 1990; p 859-870.

(S12) Roth, W. A. Zur Thermochemie des Chlors und der unterchlorigen Säure. *Z. Phys. Chem. Abt. A* **1929,** *145*, 289-297.